

# Theoretical interpretation of Pass 8 Fermi-LAT $e^+ + e^-$ data

---

**Andrea Vittino\***

*Physik-Department T30D, Technische Universität München, James-Franck Straße 1, D-85748 Garching, Germany*

*E-mail:* [andrea.vittino@tum.de](mailto:andrea.vittino@tum.de)

**Mattia Di Mauro**

*W. W. Hansen Experimental Physics Laboratory, Kavli Institute for Particle Astrophysics and Cosmology, Department of Physics and SLAC National Accelerator Laboratory, Stanford University, Stanford, CA 94305, USA*

*E-mail:* [mdimauro@slac.stanford.edu](mailto:mdimauro@slac.stanford.edu)

**Silvia Manconi**

*Department of Physics, University of Torino and Istituto Nazionale di Fisica Nucleare, via P. Giuria 1, 10125 Torino, Italy,*

*E-mail:* [manconi@to.infn.it](mailto:manconi@to.infn.it)

**Fiorenza Donato**

*Department of Physics, University of Torino and Istituto Nazionale di Fisica Nucleare, via P. Giuria 1, 10125 Torino, Italy,*

*E-mail:* [donato@to.infn.it](mailto:donato@to.infn.it)

**Nicolao Fornengo**

*Department of Physics, University of Torino and Istituto Nazionale di Fisica Nucleare, via P. Giuria 1, 10125 Torino, Italy,*

*E-mail:* [fornengo@to.infn.it](mailto:fornengo@to.infn.it)

The Fermi-LAT Collaboration has recently reported a new measurement of the inclusive cosmic-ray positron and electron spectrum in the energy range between 7 GeV and 2 TeV, obtained with almost seven years of all sky data processed with the Pass 8 event reconstruction. Here we discuss several interpretations of these results within a model where electrons and positrons are emitted by supernova remnants (SNRs) and pulsar wind nebulae (PWNe) or produced by the collision of cosmic rays with the interstellar medium. In particular, we study the emission from PWNe in relation to the limits set by the AMS-02 measurement of the positron flux. We investigate in a quantitative way the interplay between far and local SNRs by focusing on the impact of the radio constraints on the emission of electrons from the Vela SNR (which is possibly the main contributor at high energies). Furthermore, we discuss the possibility to exploit the features of the Fermi-LAT data to deduce some distinctive properties of the SNR electron spectrum at the injection, in view of the uncertainties associated to the modelling of cosmic-ray propagation in the Galaxy.

*35th International Cosmic Ray Conference — ICRC2017*

*10–20 July, 2017*

*Bexco, Busan, Korea*

---

\*Speaker.

## 1. Introduction

Cosmic-ray (CR) leptons represent an important channel for astroparticle physics investigations, in particular for what concerns the topic of CR production and acceleration, even in connection with the search for indirect dark matter signatures.

The Fermi-LAT Collaboration has recently published the results of a measurement of the inclusive CR positron and electron ( $e^+ + e^-$ ) spectrum and anisotropy in the energy range between 7 GeV and 2 TeV performed with the Pass 8 event reconstruction of almost seven years of data [1, 2]. These data seem to hint at the presence of a hardening of the lepton spectrum at  $E_b = (53 \pm 8)$  GeV with the spectral indices below and above the break being  $\gamma = (3.21 \pm 0.02)$  and  $\gamma = (3.07 \pm 0.02)$ , respectively.

As discussed in [1], the existence of this spectral break is still not certain, given its low statistical significance once that the systematic uncertainties characterising the Fermi-LAT measurement are taken into account. With this being considered, in this work we assume that this feature is real and we explore the consequences that it could have in the framework of the model proposed in [3, 4, 5].

This proceeding, which is based on [6], is organized as follows: in Section 2, we illustrate the main features of our model for what concerns the sources of CR leptons and their Galactic transport; in Section 3 we describe the approach followed in our analysis and we present our results, while in Section 4 we discuss our conclusions.

## 2. Our setup

### 2.1 Sources of CR leptons

In our model, CR leptons are produced by three sources: Supernova Remnants (SNRs), Pulsar Wind Nebulae (PWNe) and spallation reactions of primary CRs impinging on the interstellar gas (the so-called secondary production). SNRs accelerate particles that are already present in the interstellar medium and are therefore considered to be mainly a source of electrons, while PWNe may produce and accelerate both electrons and positrons in the electromagnetic processes accompanying the spin-down of pulsars. Spallation processes involve both electrons and positrons, the latter being the dominant species because of charge conservation in the collisions (since primary CRs are mainly protons).

For both SNRs and PNWe we assume the released spectrum to be a power-law with an exponential cut-off:

$$Q(E) = Q_0 \left( \frac{E}{E_0} \right)^{-\gamma} e^{-\frac{E}{E_c}}. \quad (2.1)$$

For both categories of sources the cut-off energy is fixed at  $E_c = 5$  TeV.

In the case of SNRs, we separate sources into two categories: far SNRs and local SNRs, depending on their distance from Earth being greater or less than a scale-distance  $R_{\text{cut}}$  which is treated as a free parameter and varies from case to case. Far SNRs are treated as a smooth distribution of sources characterized by the spatial distribution  $\rho(r, z) = \rho_0 f(r) e^{-\frac{|z|}{z_0}}$ , with  $z_0 = 0.1$  kpc and  $\rho_0 =$

$0.007 \text{ kpc}^{-3}$ , while  $f(r) = \left(\frac{r}{r_\odot}\right)^{1.09} e^{-3.87 \frac{r-r_\odot}{r_\odot}}$  is the SNR radial distribution taken from [7], with  $r_\odot = 8.33 \text{ kpc}$  being the Galactocentric radius of the Sun. Local SNRs, on the other hand, are treated as point-like sources, whose distances and ages are taken from the Green catalogue [8].

In the discussion of our analyses that will be conducted in next Section, the normalization of the far SNR spectrum, will be expressed in terms of the total energy emitted by the SNR in the form of electrons (under the assumption that the Supernova explosion rate is 1 per century), while the normalization of the flux from local SNRs will be related to their radio emission (see the discussion in Section 4.1 of [9]). Concerning the spectral index  $\gamma_{\text{SNR}}$ , in the case of far SNRs it will be treated as a free parameter of the fit, while in the case of local sources it will be related to the index  $\alpha$  of the synchrotron emission, by the well-known synchrotron relation:  $\gamma_{\text{SNR}} = 2\alpha + 1$ .

In the case of PWNe, the normalization of the spectrum  $Q_{0,\text{PWN}}$  is related to the spin-down energy of the pulsar,  $W_0$  (which is typically reported in pulsars catalogues), through the following relation:

$$\int_{E_{\min}}^{\infty} dE E Q(E) = \eta_{\text{PWN}} W_0, \quad (2.2)$$

where  $\eta_{\text{PWN}} \in [0, 1]$  represents the efficiency of the PWN, which is the fraction of the spin-down energy that is converted into  $e^\pm$  pairs. In all analyses described in the following, the lepton flux produced by PWNe is intended as the cumulative flux emitted by all the sources listed in the ATNF catalogue: specifically, we determine the signal emitted by each source (which is treated as a point-like source) by taking its age, distance and spin-down energy from the ATNF catalogue and by plugging these quantities into Eqs. (2.1,2.2). Moreover, in the following we will always assume that all the PWNe share the same values for the  $\eta_{\text{PWN}}$  and  $\gamma_{\text{PWN}}$  parameters, which will be free parameters in all our fits.

Concerning the electron and positron source terms associated to secondary production, they can be written as:

$$Q_{\text{sec}}(\mathbf{x}, E_e) = 4\pi \sum_{i,j} \int \Phi_{\text{CR},i}(\mathbf{x}, E_{\text{CR}}) \left. \frac{d\sigma}{dE_e} \right|_{i,j} (E_{\text{CR}}, E_e) n_{\text{ISM},j} dE_{\text{CR}}, \quad (2.3)$$

where the index  $i$  denotes the primary CR species, while  $j$  refers to the target nuclei of the interstellar medium. The quantities  $\Phi_{\text{CR},i}$  represent the primary CR flux densities per unit of energy and they are inferred by means of a fit to AMS-02 data (as detailed in [3]), while the terms  $n_{\text{ISM},j}$  are the target nuclei volume densities, which are assumed to be uniform ( $n_{\text{H}} = 0.9 \text{ cm}^{-3}$  for hydrogen and  $n_{\text{He}} = 0.1 \text{ cm}^{-3}$  for helium).  $\mathbf{x}$  is the position vector in the Galaxy and  $d\sigma/dE_e|_{i,j}$  is the differential cross section associated to the electron and positron production in the spallation reaction under consideration [10]. In the analyses described in the following, we will associate a free normalization  $q$  to secondary emission, in order to account for uncertainties in the modelling of the different ingredients that appear in Eq. (2.3).

## 2.2 Transport of CR leptons across the Galaxy

The transport of CR electrons and positrons from their source to the observer is described in terms of a transport equation:

$$\partial_t \psi - \nabla \cdot \{K(E) \nabla \psi\} + \partial_E \{b(E) \psi\} = Q(E, \mathbf{x}, t) \quad (2.4)$$

prop. model	$\eta_{\text{PWN}}$	$\gamma_{\text{PWN}}$	$E_{\text{tot,SNR}} [10^{48} \text{ erg}]$	$\gamma_{\text{SNR}}$	$q$	$\chi_{\text{red}}^2$ (38 d.o.f.)
<b>Without AMS-02 priors</b>						
MED	$0.059 \pm 0.009$	$1.45 \pm 0.03$	$5.67^{+0.3}_{-0.3}$	$2.44^{+0.05}_{-0.04}$	2.0	0.68
MAX	$0.049 \pm 0.003$	$1.39 \pm 0.02$	$12.5^{+0.2}_{-0.3}$	2.50	2.0	0.94
<b>With AMS-02 priors</b>						
MED	0.0476	1.72	$5.18^{+0.21}_{-0.20}$	$2.410^{+0.009}_{-0.009}$	1.06	3.0
MAX	0.0826	1.83	$14.0^{+0.6}_{-0.6}$	$2.542^{+0.009}_{-0.009}$	1.84	1.6

**Table 1:** Best-fit parameters obtained by fitting the *Fermi*-LAT  $e^+ + e^-$  spectrum in the framework of the MED and MAX propagation models and by assuming that all SNRs are described by the smooth distribution taken from [7]. The top and bottom half of the Table represents the results obtained by not taking and by taking into account the bounds coming from AMS-02 positron data, respectively. Those best fit values that fall at the extremes of the prior are reported here without uncertainty.

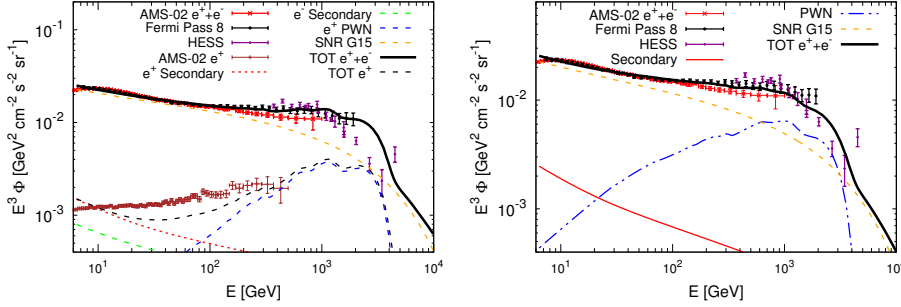


**Figure 1:** The  $e^+ + e^-$  spectrum predicted by the model under consideration (see text for details) and for the MAX propagation model is here shown in comparison with experimental data. The different lines represent the different contribution to the total emission, as reported in the legend of the plot. The left (right) panel correspond to the case where the prior arising from AMS-02 positron data are not taken (are taken) into account in the fit.

where  $K(E)$  is the spatial diffusion coefficient, modelled as a power-law in the particle rigidity  $K(E) = \beta K_0 (R/1\text{GV})^\delta \simeq K_0 (E/1\text{GeV})^\delta$ , while  $b(E)$  is the energy loss term, which takes into account synchrotron emission and inverse Compton scattering, the other processes (bremsstrahlung, ionization and Coulomb losses) being subdominant at the energies which are of interest here [11]. The technique used to solve Eq. (2.4) is the semi-analytical method of the Green function, which is extensively described in [9], to which we address the reader for all the details. In the following, we consider two sets of propagation parameters, the MED and MAX models, derived in the analysis reported in [12].

### 3. Analysis and results

#### 3.1 Smooth distribution of SNRs

We consider here a situation in which all the SNRs are treated as a smooth distribution of sources. In other words, we set the  $R_{\text{cut}}$  parameter, introduced in the previous Section, to zero. Considering also the emission from PWNe and from spallation reactions, the set of free parameters that characterise this analysis is  $\{\eta_{\text{PWN}}, \gamma_{\text{PWN}}, q, E_{\text{tot,SNR}}, \gamma_{\text{SNR}}\}$ .

We perform the fit of *Fermi*-LAT data under two different conditions: first by letting the parameters describing the positron emission by PWNe and spallation processes ( $\eta_{\text{PWN}}, \gamma_{\text{PWN}}$  and  $q$ )

free to vary, and then by imposing on their range of variability a prior that arises from the requirement that the positron flux predicted by the model is compatible (at a  $2\sigma$  C.L.) with the data reported by AMS-02 in [13].

The best-fit configurations that we obtain are reported in Table 1, while Fig. 1 shows the predicted lepton flux obtained with the MAX propagation model, in comparison with AMS-02 and Fermi-LAT data. It is clear that the model can adequately fit Fermi-LAT data only if AMS-02 constraints on the PWNe emission are not taken into account. If, on the contrary, the AMS-02 prior on  $\eta_{\text{PWN}}$ ,  $\gamma_{\text{PWN}}$  and  $q$  is implemented, the contribution from PWNe becomes more important, in particular at low/intermediate energies<sup>1</sup> and this affects the contribution from SNRs. As a consequence, the model under-predicts data at energies above 250 GeV.

By looking at the best-fit configurations reported in Table 1 (and this will be the case also for the results reported in the next Sections) one can see that the best-fit values that we obtain for the parameter  $E_{\text{tot,SNR}}$  are rather large. In fact, having  $E_{\text{tot,SNR}} \approx 10^{49}$  erg implies that a fraction  $10^{-2}$  of the typical kinetic energy that is released in a Supernova explosion is converted into  $e^\pm$  pairs. This is in tension with typical values that are assumed for this fraction, which are around  $10^{-5} \div 10^{-4}$  (see the discussion in [9]). While an accurate study on this point would represent an important addition to our investigations, it is also important to point out that  $E_{\text{tot,SNR}}$  is inversely proportional to the rate of Supernova explosions  $R$ . In this work we are assuming  $R = 1$ , which is a rather low value if compared to the ones that are often quoted in literature (as an example in [9] it was assumed  $R = 4$ ). In addition,  $E_{\text{tot,SNR}}$  strongly depends on the behaviour of the spatial distribution of SNRs which, as discussed in [9], can exhibit large fluctuations (for example, by around a factor of 2 in the local neighbourhood). Lastly, as manifest from Table 1, the best-fit value of  $E_{\text{tot,SNR}}$  depends significantly on the Galactic propagation setup that is used. Such dependence could be even stronger if one would consider propagation models where the assumption of a uniform and isotropic diffusion is relaxed.

### 3.2 The contribution from local SNRs

In order to find a better agreement with Fermi-LAT data, we modify the model described above by adopting a different treatment of the SNR contribution. In particular, we treat local SNRs as a different class of (point-like) sources. As discussed above, this is done by acting on the  $R_{\text{cut}}$  parameter, and in particular we set  $R_{\text{cut}} = 0.7$  kpc (we address the reader to [6] for the results obtained with different values of  $R_{\text{cut}}$ ). Among the local sources, a dominant role is expected to be played by the Vela SNR. Because of this, while the magnetic fields of the local SNRs are assumed to be the same for all the sources, we let the Vela magnetic field free to vary. The set of parameters that determine the total lepton emission in this analysis is thus:  $\{\eta_{\text{PWN}}, \gamma_{\text{PWN}}, q, E_{\text{tot,SNR}}, \gamma_{\text{SNR}}, B_{\text{near}}, B_{\text{Vela}}\}$ . The parameters  $\eta_{\text{PWN}}$ ,  $\gamma_{\text{PWN}}$  and  $q$  are constrained to be in a range compatible with AMS-02 positron data. Concerning the parameters of local SNRs,  $B_{\text{Vela}}$  is left free and  $B_{\text{near}} \in [20, 60] \mu\text{G}$  [14], while the spectral indices are taken to be compatible with synchrotron emission as detailed in Section 2 (this implies  $\gamma_{\text{Vela}} = 2.5$ ). The best-fit configurations obtained by fitting Fermi-LAT data within this model are reported in the top half of Table 2 and the corresponding lepton flux is show in the left

<sup>1</sup>This happens because, as it can be seen from the left panel of Fig. 1, when all the parameters are left unconstrained, the model under-predicts the positron flux with respect to AMS-02 data.

prop. model	$\eta_{\text{PWN}}$	$\gamma_{\text{PWN}}$	$E_{\text{tot,SNR}} [10^{48} \text{ erg}]$	$\gamma_{\text{SNR}}$	$q$	$\gamma_{\text{Vela}}$	$B_{\text{Vela}} [\mu\text{G}]$	$B_{\text{near}} [\mu\text{G}]$	$\chi_{\text{red}}^2$ (38 d.o.f.)
<b>Without constraints on <math>B_{\text{Vela}}</math></b>									
MED	0.0476	1.72	$9.4^{+0.7}_{-0.6}$	$2.392^{+0.006}_{-0.005}$	1.06	2.5	$6.3^{+0.3}_{-0.3}$	20	0.75
MAX	0.0693	1.83	$23.6^{+0.3}_{-0.2}$	$2.563^{+0.002}_{-0.002}$	1.55	2.5	$5.7^{+0.3}_{-0.3}$	20	0.39
<b>With constraints on <math>B_{\text{Vela}}</math></b>									
MED	0.0476	1.72	$8.26^{+0.45}_{-0.40}$	$2.358^{+0.009}_{-0.008}$	1.06	2.29	38	$43 \pm 3$	2.6
MAX	0.0830	1.83	$14.7^{+0.8}_{-0.7}$	$2.462^{+0.011}_{-0.010}$	1.84	2.29	38	$53 \pm 4$	1.52

**Table 2:** Best-fit parameters obtained by fitting the *Fermi*-LAT  $e^+ + e^-$  spectrum in the framework of the MED and MAX propagation models and by taking into account the contribution from far and local SNRs with the method described in the text. The top and bottom half of the Table represents the results obtained by not taking and by taking into account the bounds on the Vela magnetic field, respectively. Those best fit values that fall at the extremes of the prior are reported here without uncertainty.

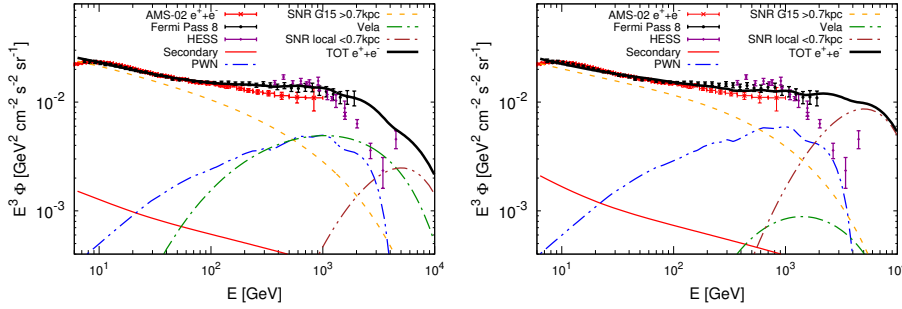


**Figure 2:** The  $e^+ + e^-$  spectrum predicted by the model under consideration (see text for details) and for the MAX propagation model is here shown in comparison with experimental data. The different lines represent the different contribution to the total emission, as reported in the legend of the plot. The left (right) panel correspond to the case where the prior on the Vela magnetic field are not taken (are taken) into account in the fit.

panel of Fig. 2. It is clear that with this treatment of local SNRs the model is in good agreement with data, also at high energies.

In order to further investigate the validity of this model, we constrain the magnetic field of Vela to be compatible with the observed values. In particular, we require that the parameters that rule the emission from Vela do not deviate by more than  $2\sigma$  from the values inferred from the analysis conducted in [15]. This means that we require  $\gamma_{\text{Vela}} \in [2.29, 2.65]$  and  $Q_{0,\text{Vela}} \in [ , ]^2$ . The best-fit configurations obtained in this case are reported in the bottom half of Table 2 and the corresponding flux is shown in the right panel of Fig. 2. It can be seen that the fit worsens: in particular, the constraints on the emission from Vela make the lepton flux produced by this source about one order of magnitude smaller and because of this the model under-predicts data at energies between 200 GeV and 1 TeV.

### 3.3 A spectral break in the injection

In this analysis we follow a different approach in trying to find a better agreement with the hint of a spectral break present in *Fermi*-LAT data. Specifically, we introduce a break in the electron

<sup>2</sup>These bounds on  $Q_{0,\text{Vela}}$  arise from the constraints on  $E_{\text{tot,Vela}}$  reported in [15] under the assumption that  $B_{\text{Vela}} = 38 \mu\text{G}$ , as detailed in [6].

	$\eta_{\text{PWN}}$	$\gamma_{\text{PWN}}$	$E_{\text{tot,SNR}} [10^{48} \text{ erg}]$	$\gamma_{1,\text{SNR}}$	$\gamma_{2,\text{SNR}}$	$E_b^Q [\text{GeV}]$	q	$\chi_{\text{red}}^2$ (38 d.o.f.)
MED	0.0476	1.72	$12.5^{+0.9}_{-0.8}$	$2.608^{+0.011}_{-0.010}$	$2.185^{+0.018}_{-0.016}$	$100^{+15}_{-15}$	1.063	0.28
MAX	0.0693	1.83	$26.6^{+0.4}_{-0.4}$	$2.673^{+0.008}_{-0.007}$	$2.378^{+0.017}_{-0.016}$	$100^{+15}_{-15}$	1.84	0.24

**Table 3:** *Analysis-4.* Best-fit parameters obtained by fitting the *Fermi*-LAT  $e^+ + e^-$  spectrum in the framework of the MED and MAX propagation models and by assuming a break in the injection spectrum from SNRs. Those best fit values that fall at the extremes of the prior are reported here without uncertainty.

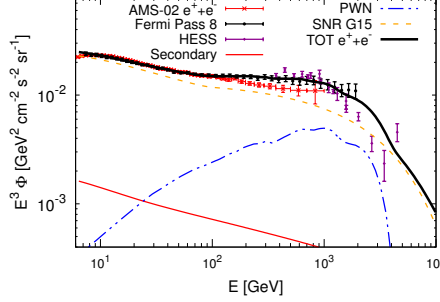


**Figure 3:** The  $e^+ + e^-$  spectrum predicted by the model under consideration (see text for details) and for the MAX propagation model is here shown in comparison with experimental data. The different lines represent the different contribution to the total emission, as reported in the legend of the plot.

spectrum injected by SNRs, which could be seen as due to the details of diffusive shock acceleration mechanisms in SNR shocks or to the contribution from a different SNR population.

We treat SNRs as a smooth distribution of sources, i.e. we set  $R_{\text{cut}} = 0$ ; the source term is assumed to be a power-law with exponential cut-off as in Eq. (2.1), with spectral indices  $\gamma_{1,\text{SNR}}$  and  $\gamma_{2,\text{SNR}}$  below and above the break, whose energy is denoted with  $E_b^Q$ . Secondary emission and the contribution from PWNe are set to be compatible with the AMS-02 positron constraints. The free parameters that characterize this analysis are therefore  $\{E_{\text{tot,SNR}}, \gamma_{1,\text{SNR}}, \gamma_{2,\text{SNR}}, E_b^Q\}$ . The best-fit configuration and the associated chi-square are reported in Table 3, while the lepton flux predicted by this model for the MAX propagation setup is shown in Fig. 3. As it can be clearly seen, the agreement with data is now remarkably good.

## 4. Conclusions

In this work we have performed several fits of *Fermi*-LAT lepton data under a variety of scenarios. In particular, we have shown how with a smooth distribution of SNRs, the agreement with data is good only if one does not take into account the priors on PWNe properties that can be inferred from AMS-02 positron measurements. We have seen how separating SNRs into far and local sources, with the properties of the local sources taken directly from catalogues can improve the agreement with data, but the fit is good only if one does not take into account constraints on the emission from local sources that can come from the radio emission. As a last case, we have illustrated how a spectral break in the injection spectrum can improve the results of the fit.

## Acknowledgements

The *Fermi*-LAT Collaboration acknowledges support for LAT development, operation and

data analysis from NASA and DOE (United States), CEA/Irfu and IN2P3/CNRS (France), ASI and INFN (Italy), MEXT, KEK, and JAXA (Japan), and the K.A. Wallenberg Foundation, the Swedish Research Council and the National Space Board (Sweden). Science analysis support in the operations phase from INAF (Italy) and CNES (France) is also gratefully acknowledged.

## References

- [1] FERMI-LAT collaboration, S. Abdollahi et al., *Cosmic-ray electron+positron spectrum from 7 GeV to 2 TeV with the Fermi Large Area Telescope*, *ArXiv e-prints* (Apr., 2017) , [[1704.07195](#)].
- [2] FERMI-LAT collaboration, S. Abdollahi et al., *Search for cosmic-ray electron and positron anisotropies with seven years of fermi large area telescope data*, *Phys.Rev.Lett.* **118** (Mar, 2017) 091103.
- [3] M. Di Mauro, F. Donato, N. Fornengo et al., *Interpretation of AMS-02 electrons and positrons data*, *JCAP* **1404** (2014) 006, [[1402.0321](#)].
- [4] M. Di Mauro, F. Donato, N. Fornengo et al., *Dark matter vs. astrophysics in the interpretation of AMS-02 electron and positron data*, *JCAP* **1605** (2016) 031, [[1507.07001](#)].
- [5] S. Manconi, M. Di Mauro and F. Donato, *Dipole anisotropy in cosmic electrons and positrons: inspection on local sources*, *JCAP* **1701** (2017) 006, [[1611.06237](#)].
- [6] M. Di Mauro et al., *Theoretical interpretation of Pass 8 Fermi-LAT  $e^+ + e^-$  data*, [1703.00460](#).
- [7] D. A. Green, *Constraints on the distribution of supernova remnants with Galactocentric radius*, *MNRAS* **454** (Dec., 2015) 1517–1524, [[1508.02931](#)].
- [8] D. A. Green, *A catalogue of 294 Galactic supernova remnants*, *Bull. Astron. Soc. India* **42** (2014) 47, [[1409.0637](#)].
- [9] T. Delahaye, J. Lavalley, R. Lineros et al., *Galactic electrons and positrons at the Earth: new estimate of the primary and secondary fluxes*, *A&A* **524** (Dec., 2010) A51, [[1002.1910](#)].
- [10] T. Kamae, N. Karlsson, T. Mizuno et al., *Parameterization of  $\gamma$ ,  $e^{+/-}$ , and Neutrino Spectra Produced by  $p$ - $p$  Interaction in Astronomical Environments*, *ApJ* **647** (Aug., 2006) 692–708, [[astro-ph/0605581](#)].
- [11] T. Delahaye, R. Lineros, F. Donato, N. Fornengo, J. Lavalley, P. Salati et al., *Galactic secondary positron flux at the Earth*, *A&A* **501** (July, 2009) 821–833, [[0809.5268](#)].
- [12] F. Donato, N. Fornengo, D. Maurin et al., *Antiprotons in cosmic rays from neutralino annihilation*, *Phys.Rev.D* **69** (2004) 063501, [[astro-ph/0306207](#)].
- [13] AMS collaboration, M. Aguilar et al., *Electron and Positron Fluxes in Primary Cosmic Rays Measured with the Alpha Magnetic Spectrometer on the International Space Station*, *Phys.Rev.Lett.* **113** (Sept., 2014) 121102.
- [14] H. Katagiri, L. Tibaldo, J. Ballet et al., *Fermi large area telescope observations of the cygnus loop supernova remnant*, *ApJ* **741** (2011) 44.
- [15] I. Sushch and B. Hnatyk, *Modelling of the radio emission from the Vela supernova remnant*, *A&A* **561** (2014) A139, [[1312.0777](#)].